PHYSICAL REVIEW B **82**, 020402(R) (2010)

Role of interface alloying in the exchange bias of Fe/Cr bilayers

S. Rizwan Ali,[1,*] M. Bilal Janjua,[1] M. Fecioru-Morariu,[1,†] D. Lott,[2] C. J. P. Smits,[1,‡] and G. Güntherodt[1]
[1]*Physikalisches Institut (IIA), RWTH Aachen University, 52056 Aachen, Germany*
[2]*GKSS Research Centre, 21502 Geesthacht, Germany*

(Received 11 January 2010; revised manuscript received 16 May 2010; published 7 July 2010)

The exchange bias field, H_{EB}, in polycrystalline Fe/Cr bilayers exhibits a temperature-driven sign reversal due to an Fe-Cr spin glass (SG). Interdiffusion and alloying at the Fe/Cr interface drive Cr into a re-entrant Fe-cluster SG phase, stabilized after field cooling below the SG transition temperature. The temperature tuning through the SG-to-antiferromagnet phases yields at the interface to the Fe overlayer a sign change in the exchange couplings and hence of H_{EB}. The H_{EB} of samples containing the intentionally deposited Fe-Cr SG alloy underneath the Fe overlayer shows all the features of H_{EB} observed in the Fe/Cr bilayers in support of our arguments.

DOI: 10.1103/PhysRevB.82.020402 PACS number(s): 75.70.Cn, 75.50.Lk, 75.50.Bb

The discovery of antiferromagnetic coupling between two Fe layers in Fe/Cr/Fe trilayers[1] and of giant magnetoresistance (GMR) in Fe/Cr multilayers[2] has stimulated widespread research. Part of this was the oscillatory interlayer exchange coupling and the bulk vs interface electron scattering in these systems. A number of anomalies in the magnetic properties of these multilayers, however, has also arisen mainly because of the presence of interface alloying.[3–5] In particular, the GMR in Fe/Cr multilayers has been found to be sensitive to interface alloying.[6]

The interface of a ferromagnet (FM) with the spin-density wave (SDW) antiferromagnet (AFM) Cr (Refs. 5 and 7) has also triggered some studies of interfacial exchange coupling, i.e., the exchange bias (EB) phenomenon.[8,9] After cooling the bilayer in an external magnetic field below the Néel temperature, T_N, of the AFM, this coupling gives rise to a shift of the hysteresis loop along the magnetic field axis by the EB field, H_{EB}.[10] For epitaxial $Ni_{81}Fe_{19}$/Cr(100) bilayers a maximum of the negative H_{EB} has been found below 150 K.[8] The superimposed oscillations of H_{EB} as function of temperature have been attributed to the incommensurate SDW in the AFM Cr(100) layer. In epitaxial Fe/Cr(001) bilayers small amplitude (~1 Oe) multiple-period oscillations in both magnitude and sign of H_{EB} have been observed in its temperature dependence above 70 K.[9] These oscillations are attributed to a sinusoidally modulated Cr interfacial moment. However, the low-temperature behavior of H_{EB}, exhibiting an enhanced strength[8,9] and a sign reversal[9] has not been explained by the above models.

Here we report on systematic investigations of the low-temperature enhancement and sign change in H_{EB} in polycrystalline Fe/Cr bilayers. An explanation is given by considering an interdiffused rather than a chemically abrupt Fe/Cr interface. The H_{EB} of samples with an intentionally deposited $Cr_{1-x}Fe_x$ alloy underneath the Fe overlayer ($Cr_{1-x}Fe_x$/Fe) shows all the features of H_{EB} observed in our Fe/Cr bilayers. This similarity was observed for $0.15 \leq x \leq 0.20$, i.e., for an Fe concentration lying in the composition range of the Fe-Cr spin glass (SG).[7] At low temperature the exchange interaction between the frozen Fe clusters in the SG and the Fe overlayer is ferromagnetic which yields a negative H_{EB}. The sign change in H_{EB} with increasing temperature is attributed to a temperature-driven re-entrant phase transition in the interfacial alloy from the cluster SG to the AFM phase. The positive H_{EB} originates from the antiferromagnetic coupling between the AFM and the Fe overlayer.

A series of samples with the layer sequence, $Si/SiO_2/Cu(10\ nm)/Fe(6\ nm)/Cr(t_{Cr})/Au(5\ nm)$, with t_{Cr} varied between 10 and 40 nm (series A) was deposited by molecular-beam epitaxy (MBE) at room temperature. The Cu layer serves as buffer layer. To study the effect of growth conditions on H_{EB}, another series with identical layer sequence was grown by sputtering (series B). Atomic-force microscopy scans show that all the samples studied in the present work have a granular structure (rms roughness ~1.0 nm). Transmission electron microscopy and x-ray reflectivity reveal that the samples are polycrystalline. Magnetic characterizations were performed by superconducting quantum interference device (SQUID) magnetometry after cooling the samples from 370 K through T_N (311 K for bulk Cr) to 5 K in a cooling field (H_{CF}) of 1 kOe (unless otherwise specified). The temperature was then increased in steps (from 5 to 330 K) and a hysteresis-loop measurement was carried out for each step. We have convinced ourselves that the data are changed only slightly if the sample is warmed to 370 K and then recooled in a field before measuring each loop. The coercive fields of the hysteresis cycles H_{C1} and H_{C2} were used to estimate $H_{EB}=(H_{C1}+H_{C2})/2$.

The temperature dependence of H_{EB} is shown in Fig. 1 in the range of $5\ K \leq T \leq 300\ K$ for samples of series A [Fig. 1(a)] and series B [Fig. 1(b)]. For both series the H_{EB} is found to be negative at very low temperatures and it decreases with temperature up to a temperature T_0 at which it changes sign and passes through a positive maximum before vanishing at the blocking temperature, T_B. The low-temperature sign change and maximum of H_{EB} observed in our polycrystalline Fe/Cr bilayers are very similar to the behavior observed in epitaxial Fe/Cr bilayers.[9] However, contrary to the epitaxial bilayers we do not observe any oscillations of H_{EB} for temperatures higher than the positive maximum in Fig. 1. The reason is that the observation of oscillatory H_{EB} requires an epitaxial Cr(100) film to stabilize the SDW.[8,9] This condition is not satisfied for our polycrystalline Cr layers with a granular structure.

In a next step, we test the role of the Fe/Cr interface for EB by introducing an oxide layer as diffusion barrier at different growth stages of the bilayer. Oxygen was introduced

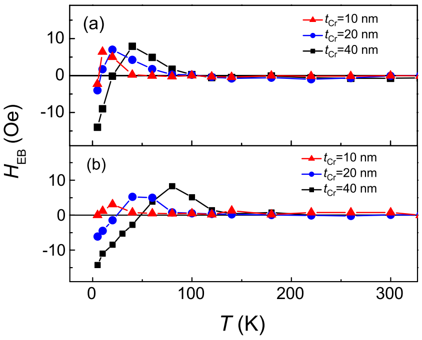

FIG. 1. (Color online) Exchange bias field H_{EB} of Fe(6 nm)/Cr(t_{Cr}) bilayers as a function of temperature T for different values of Cr thickness t_{Cr} grown by (a) molecular-beam epitaxy and (b) sputtering.

into the deposition chamber for the intentional oxidation stage. Two different Fe/Cr bilayers with t_{Cr}=40 nm were grown by sputtering at room temperature with the oxidation stages indicated by the arrows in the insets of Fig. 2. For sample-1, the oxidation was carried out after the formation of Fe/Cr interface, i.e., after the growth of 5 nm Cr on top of the Fe underlayer. The remaining 35 nm of the Cr overlayer and 5 nm of the Au cap layer were grown after recovering the vacuum. This yields an unoxidized, nominally intact Fe/Cr interface. Clearly, $H_{EB}(T)$ of sample-1 in Fig. 2(a) exhibits the sign change and positive maximum as observed in Fig. 1. On the other hand, sample-2, for which the oxidation is carried out after the growth of the Fe underlayer yielding an Fe oxide/Cr interface, exhibits no sign change with temperature [Fig. 2(b)]. The negative H_{EB} for sample-2 is attributed to the exchange interaction between Fe/Fe oxide, the latter being either antiferromagnetic α-Fe_2O_3 or FeO (Ref. 10). Clearly the nominal Fe/Cr interface is necessary for the sign reversal of $H_{EB}(T)$.

The role of interdiffusion and alloying at the Fe/Cr interface can be tested by considering the melting points of underlayer and overlayer.[4] The melting point of Fe (~1808 K) is lower than that of Cr (~2130 K) and thus the interface alloying should be significant for an Fe/Cr interface. In polycrystalline samples interfacial defects and roughness may act as nucleation centers to further enhance the interface alloying. On the other hand, no alloying should occur for the reversed interface, i.e., Cr/Fe. This is consistent with the temperature dependence of H_{EB} of the Cr (40 nm)/Fe(6 nm) bilayer shown in Fig. 3(a), which does not exhibit any sign reversal of H_{EB}. The inset of Fig. 3(a) shows the dependence of H_{EB} on H_{CF} at 5 K for an Fe(6 nm)/Cr(40 nm) bilayer and a reversed Cr (40 nm)/Fe(6 nm) bilayer sample. Obviously, the H_{EB} of the sample with the Fe/Cr interface does not depend markedly on H_{CF} whereas a clear H_{CF} driven sign reversal is observed for the Cr/Fe interface. This behavior indicates that after cooling the sample to 5 K for different values of H_{CF}, the coupling at the Fe/Cr interface is ferromagnetic. On the contrary, for the reversed Cr/Fe interface the interfacial coupling is antiferromagnetic. Such an interface undergoes with increasing H_{CF} a change in sign of H_{EB}, indicative of a change from antiferromagnetic to ferromagnetic interface coupling.[10,11] Since the nominal coupling between Fe and Cr at interfaces is antiferromagnetic,[5,12] the difference between Fe/Cr and reversed Cr/Fe interfaces is attributed to the formation of a $Cr_{1-x}Fe_x$ alloy at the Fe/Cr interface.

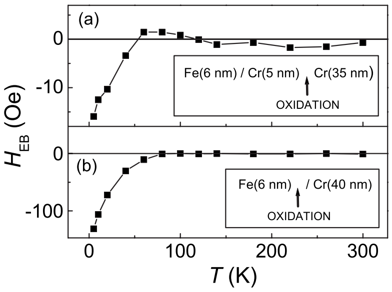

FIG. 2. Exchange bias field H_{EB} as a function of temperature T for (a) sample-1 and (b) sample-2 of the same nominal composition. Both the samples were oxidized at different growth stages as shown by the arrows in the insets in (a) and (b). Details about the sample growth are described in the text.

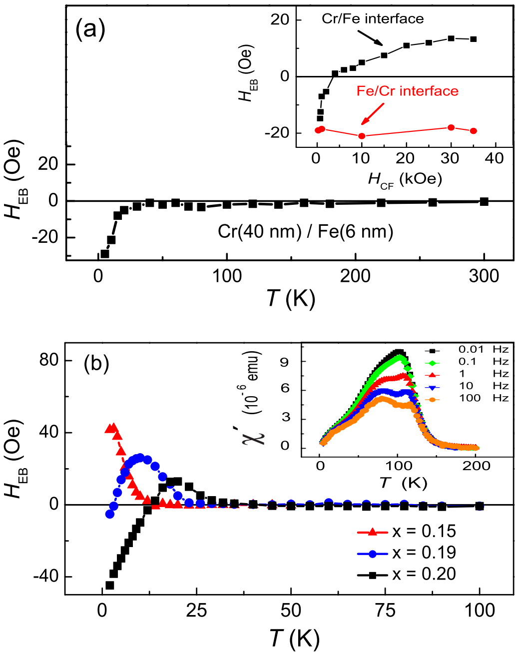

FIG. 3. (Color online) (a) Exchange bias field H_{EB} as a function of temperature T for a bilayer with a reversed Cr(40 nm)/Fe(6 nm) interface. Inset: exchange bias field H_{EB} at 5 K as a function of cooling field strength H_{CF} for bilayers with a Cr(40 nm)/Fe(6 nm) (squares) and an Fe(6 nm)/Cr(40 nm) (circles) interfaces. (b) Exchange bias field H_{EB} as a function of temperature T for bilayers containing an intentionally alloyed layer $Cr_{1-x}Fe_x$(40 nm) for different concentrations x of Fe content exchange biased by an Fe(6 nm) layer. Inset: temperature dependence of the real part of the ZFC ac susceptibility $\chi'(T)$ for a sole intentionally alloyed $Cr_{1-x}Fe_x$ layer with x=0.20 and frequencies from 0.01 Hz (squares) to 100 Hz (circles).

In order to demonstrate the effect of interface alloying on H_{EB} more clearly, a series of samples (series C) containing $Cr_{1-x}Fe_x$ alloys for values of $0.15 \leq x \leq 0.20$ underneath the interface to the Fe layer on top was grown by MBE with the layer sequence: Si/SiO_2/Cu(10 nm)/$Cr_{1-x}Fe_x$(40 nm)/Fe(6 nm)/Au(5 nm). For the deposition of the binary alloy two quartz microbalances together with a computer controlled feedback loop to the evaporation sources kept the rates (and thus the alloy composition) constant to within 1%. Note that we have deliberately chosen for these samples the reverse growth sequence with a nominal Cr/Fe type interface. As we have mentioned previously, for this growth sequence no interface alloying should occur[4] and thus the composition of the intentionally deposited $Cr_{1-x}Fe_x$ layer should not be affected by interface alloying. Figure 3(b) shows the $H_{EB}(T)$ for some selected values of $0.15 \leq x \leq 0.20$ which cover the range of the SG composition of the bulk alloys.[7] In this composition range the H_{EB} of $Cr_{1-x}Fe_x$/Fe bilayers (series C) exhibits similar features as observed for the Fe/Cr bilayers in Figs. 1(a) and 1(b) for series A and B, respectively.

For a better understanding of the origin of the observed features of H_{EB} of our samples, sole $Cr_{1-x}Fe_x$ layers of the type: Si/SiO_2/Cu(10 nm)/$Cr_{1-x}Fe_x$(40 nm)/Au(5 nm) were deposited for $x=0.19$ and 0.20 under the same conditions as we used for series C. Low field magnetization (M) and ac susceptibility (ACS) of these alloy films were measured as a function of temperature by SQUID magnetometry. The $M(T)$ measurements (not shown here) reveal a strong irreversibility between field-cooled (FC) and zero-field-cooled (ZFC) curves indicating the onset of a SG transition[13] in both samples. The temperature at which the irreversibility appears was (50 ± 10) K for $x=0.19$ and (65 ± 10) K for $x=0.20$. We denote this temperature as T_{RSG} which will be defined below. The inset of Fig. 3(b) shows the temperature dependence of the real part of the ZFC ACS, χ', for a sole intentionally alloyed $Cr_{1-x}Fe_x$ layer with $x=0.20$ from 0.01 Hz (squares) to 100 Hz (circles). Clearly, $\chi'(T)$ exhibits a peak for 0.01 and 0.1 Hz which changes with increasing frequency to a plateau with a double peak structure. The high-temperature peak occurs at a temperature T^* near which the system undergoes with increasing temperature a transition from the ordered AFM or FM phases into the disordered paramagnetic phase. The low-temperature peak is with decreasing temperature a signature of a re-entrant SG (RSG) transition from the ordered AFM or FM phases into the cluster SG phase[13–15] near its transition temperature T_{RSG}.

According to the magnetic phase diagram of the bulk $Cr_{1-x}Fe_x$ alloy a SG composition lying near the boundaries to the AFM and FM phases shows temperature-driven RSG transitions into the respective AFM and FM phases.[16–18] These RSG transitions are not sharp on the microscopic scale, i.e., the system can be described neither by a single Curie temperature T_C or T_N nor by one value of T_{RSG}.[17,18] This is because of the fact that the magnetic properties of the $Cr_{1-x}Fe_x$ alloy depend very sensitively on the local concentration of Fe atoms or Fe clusters in the Cr matrix.[17,18] The nonuniform distribution of Fe atoms due to clustering in the $Cr_{1-x}Fe_x$ alloy would yield in some local regions a SG composition close to that near the FM-RSG phase boundary. In these regions the alloy supports a RSG-to-FM transition upon increasing the temperature.[17] Similarly in Fe deficient regions, the alloy composition will be closer to that near the AFM-RSG phase boundary and thus a temperature-driven RSG-to-AFM transition is favored.[18] The formation of the RSG state upon cooling can be understood as follows. By lowering the temperature below T^*, a mixture of ferromagnetic and superparamagnetic Fe clusters is formed. At lower temperature ($T_{RSG} \leq T \leq T^*$) the state becomes a mixture of ferromagnetic clusters distributed in the AFM Cr matrix. By further decreasing the temperature ($T \leq T_{RSG}$) the Fe clusters freeze out such that the long-range order decreases and a RSG state evolves.[19] Competing exchange interactions are considered to be at the origin of these RSG transitions in the CrFe alloy[20] as well as of the sign change in H_{EB}. The Fe-Fe interaction is ferromagnetic whereas Cr-Cr and Cr-Fe interactions are antiferromagnetic.

In the light of the above arguments the temperature dependence of H_{EB} of our $Cr_{1-x}Fe_x$/Fe bilayer system can be interpreted as follows. In the field cooling process, as the $Cr_{1-x}Fe_x$ alloy undergoes a RSG transition at $T=T_{RSG}$, the Fe clusters in the RSG become frozen, giving a net ferromagnetic coupling with the Fe overlayer near its interface. The degree by which a cluster is coupled to the surrounding moments within the glass will depend on its size, shape, and the details of the local magnetic anisotropy. Clusters which are more strongly coupled due to their large anisotropy and with their net moments blocked will remain largely pinned during the reversal of the FM layer, yielding negative H_{EB}.[21] With increasing temperature, the effective ferromagnetic interfacial coupling decreases as T_{RSG} is approached where the alloy undergoes a RSG-to-FM and RSG-to-AFM phase transitions. However, due to the Cr rich alloy composition, local regions favoring a RSG-to-AFM transition will dominate. Above this transition temperature in the AFM-dominated regions the uncompensated moments of the antiferromagnetic Cr prefer antiparallel alignment with the Fe layer at the interface.[5,12] Hence, there will be a sign reversal temperature above which the antiferromagnetic coupling will dominate at the Fe/Cr interface. Consequently, with increasing temperature the H_{EB} changes sign from negative to positive. The gradual rise to a positive maximum is due to the inhomogeneous composition of the alloy and the gradual disappearance of the FM clusters. Thereafter, the positive H_{EB} decreases because of the disappearance of the AFM order near T_B, where the H_{EB} vanishes. T_B is significantly lower than the bulk T_N since the addition of Fe to Cr leads to a decrease in T_N.[7] Moreover, in thin films the T_B is generally lower than the bulk T_N because of finite-size effects.[22]

There is some similarity of the sign reversal of H_{EB} of the $Cr_{1-x}Fe_x$/Fe bilayers to the one observed by Ali *et al.*[23] for a canonical SG ($\underline{Cu}$Mn) exchange biased to a ferromagnet (Co). They attributed the sign reversal of H_{EB} to long-range RKKY interactions that lead to the SG state in dilute $\underline{Cu}$Mn. However, the RSG state we have discussed above differs from that of a canonical SG, which contains isolated, randomly oriented magnetic moments dispersed in the metallic matrix. On the other hand, in the RSG the presence of ensembles of magnetic atoms or clusters, with a distribution of size, shape, and magnetic anisotropies, presents a more complex situation and requires a different quantitative description. The latter we would like to stimulate by this work.

Recently, Lund and Leighton[24] have shown that a SG phase, which is formed due to alloying at the NiMn/Ni interface, affects the temperature dependence of H_{EB} and leads to its enhancement. However, in our case, competing exchange interactions and thus different phases in the cluster SG phase, which is formed at the Fe/Cr interface, yield not only an enhancement of H_{EB} but also cause its sign reversal at low temperature. We believe that this constitutes a topical and intriguing example of temperature tuning H_{EB} involving competing magnetic phases of the Fe-Cr alloy.

A sign change in H_{EB} has been observed by Gredig *et al.*[25] in the Co/CoO bilayer system. It is interpreted by a model based on the nonmonotonic temperature dependence of the right-hand coercivity exhibiting a peak below T_B. This behavior is attributed to a disordered interface due to reversed AFM grains. The Co/CoO bilayer system investigated by Gredig *et al.*[25] differs from our Fe/Cr bilayer sample because the latter exhibits interdiffusion and alloying at the Fe/Cr interface as well as SG formation. Moreover, we observe a nonmonotonic temperature dependence and a peak below T_B in both the right-hand and left-hand coercivities (inset of Fig. 4). A similar behavior of the coercive fields is also observed by Ali *et al.* (Ref. 23 and its supplementary information) in another SG system, Co/CuMn, which we have discussed above. The nonmonotonic temperature dependence of the left-hand coercivity of our system cannot be accounted for by the model proposed by Gredig *et al.*[25] Thus, we developed an adequate model considering the composition and temperature-dependent phase diagram of a cluster SG, explaining the underlying mechanism of the sign reversal of H_{EB} in our Fe/Cr bilayers. There are other instances of sign reversal of H_{EB} in the literature, such as, FeF_2/Fe by Nogues *et al.*[11] However, the qualitative features of our data differ from these cases.

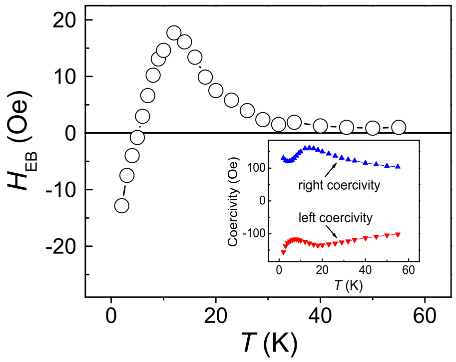

FIG. 4. (Color online) Temperature dependence of the exchange bias field H_{EB} of an Fe(6 nm)/Cr(10 nm) bilayer. Inset: temperature dependence of the left/right-hand coercivities.

In summary, the temperature-driven sign reversal of H_{EB} of polycrystalline Fe/Cr bilayers is explained by considering interface alloying and the formation of a cluster SG phase which is stabilized after field cooling. The ferromagnetic interfacial coupling between frozen Fe clusters in the SG and the Fe overlayer yields a negative H_{EB} at low temperatures. The sign reversal occurs as a consequence of a temperature-driven re-entrant cluster SG-to-AFM phase transition in the interfacial alloy. Consequently, antiferromagnetic interfacial coupling between the uncompensated Cr moments and the Fe layer yields a positive H_{EB}.

Two of the authors, S.R.A. and M.B.J., are grateful for funding by the Higher Education Commission (HEC), Government of Pakistan, under DAAD/HEC program.

---

*Corresponding author; rizwan@physik.rwth-aachen.de

†Present address: Oerlikon Solar AG, 9477 Trübbach, Switzerland.

‡Present address: OTB Solar, 5657 EB Eindhoven, The Netherlands.

[1] P. Grünberg, R. Schreiber, Y. Pang, M. B. Brodsky, and H. Sowers, Phys. Rev. Lett. **57**, 2442 (1986).
[2] M. N. Baibich, J. M. Broto, A. Fert, F. Nguyen Van Dau, F. Petroff, P. Etienne, G. Creuzet, A. Friederich, and J. Chazelas, Phys. Rev. Lett. **61**, 2472 (1988).
[3] A. Davies *et al.*, J. Magn. Magn. Mater. **165**, 82 (1997).
[4] B. Heinrich, J. F. Cochran, T. Monchesky, and R. Urban, Phys. Rev. B **59**, 14520 (1999).
[5] D. T. Pierce *et al.*, J. Magn. Magn. Mater. **200**, 290 (1999).
[6] F. Petroff *et al.*, J. Magn. Magn. Mater. **93**, 95 (1991); B. J. Daniels and B. M. Clemens, Appl. Phys. Lett. **66**, 520 (1995); M. C. Cyrille, S. Kim, M. E. Gomez, J. Santamaria, K. M. Krishnan, and I. K. Schuller, Phys. Rev. B **62**, 3361 (2000).
[7] E. Fawcett *et al.*, Rev. Mod. Phys. **66**, 25 (1994).
[8] F. Y. Yang and C. L. Chien, Phys. Rev. Lett. **90**, 147201 (2003).
[9] J. S. Parker, L. Wang, K. A. Steiner, P. A. Crowell, and C. Leighton, Phys. Rev. Lett. **97**, 227206 (2006).
[10] J. Nogués and I. K. Schuller, J. Magn. Magn. Mater. **192**, 203 (1999).
[11] J. Nogués, D. Lederman, T. J. Moran, and Ivan K. Schuller, Phys. Rev. Lett. **76**, 4624 (1996).
[12] T. G. Walker, A. W. Pang, H. Hopster, and S. F. Alvarado, Phys. Rev. Lett. **69**, 1121 (1992); C. Turtur and G. Bayreuther, *ibid.* **72**, 1557 (1994).
[13] J. A. Mydosh, *Spin Glasses: An Experimental Introduction* (Taylor & Francis, London, 1993).
[14] R. D. Shull and P. A. Beck, in *Magnetism and Magnetic Materials*, edited by C. D. Graham, G. H. Lander, and J. J. Rhyne, AIP Conf. Proc. No. 24 (AIP, New York, 1975), p. 95.
[15] G. J. Nieuwenhuys, B. H. Verbeek, and J. A. Mydosh, J. Appl. Phys. **50**, 1685 (1979).
[16] S. M. Shapiro, C. R. Fincher, A. C. Palumbo, and R. D. Parks, Phys. Rev. B **24**, 6661 (1981).
[17] S. M. Dubiel, Ch. Sauer, and W. Zinn, Phys. Rev. B **30**, 6285 (1984).
[18] S. M. Dubiel, Ch. Sauer, and W. Zinn, Phys. Rev. B **32**, 2745 (1985).
[19] N. Kunitomi *et al.*, Hyperfine Interact. **28**, 515 (1986).
[20] P. Mangin, D. Boumazouza, B. George, J. J. Rhyne, and R. W. Erwin, Phys. Rev. B **40**, 11123 (1989).
[21] C. Schlenker, S. S. P. Parkin, J. C. Scott, and K. Howard, J. Magn. Magn. Mater. **54-57**, 801 (1986).
[22] T. Ambrose and C. L. Chien, J. Appl. Phys. **83**, 6822 (1998).
[23] M. Ali *et al.*, Nature Mater. **6**, 70 (2007).
[24] M. S. Lund and C. Leighton, Phys. Rev. B **76**, 104433 (2007).
[25] T. Gredig, I. N. Krivorotov, P. Eames, and E. D. Dahlberg, Appl. Phys. Lett. **81**, 1270 (2002).